Supporting Information

Fusaristatin C, a Cyclic Lipodepsipeptide from *Pithomyces* sp. RKDO 1698

Logan W. MacIntyre[†], Douglas H. Marchbank[‡§], Hebelin Correa[§] and Russell G. Kerr[†‡§]*

[†]Department of Biomedical Sciences and [‡]Department of Chemistry, University of Prince Edward Island, 550 University Avenue, Charlottetown, PE, Canada, C1A 4P3
[§]Nautilus Biosciences Croda, Regis and Joan Duffy Research Centre, 550 University Avenue, Charlottetown, PE, Canada, C1A 4P3

*Tel: 1-902-566-0565. Fax: 1-902-566-7445. Email: rkerr@upei.ca

Supporting Information

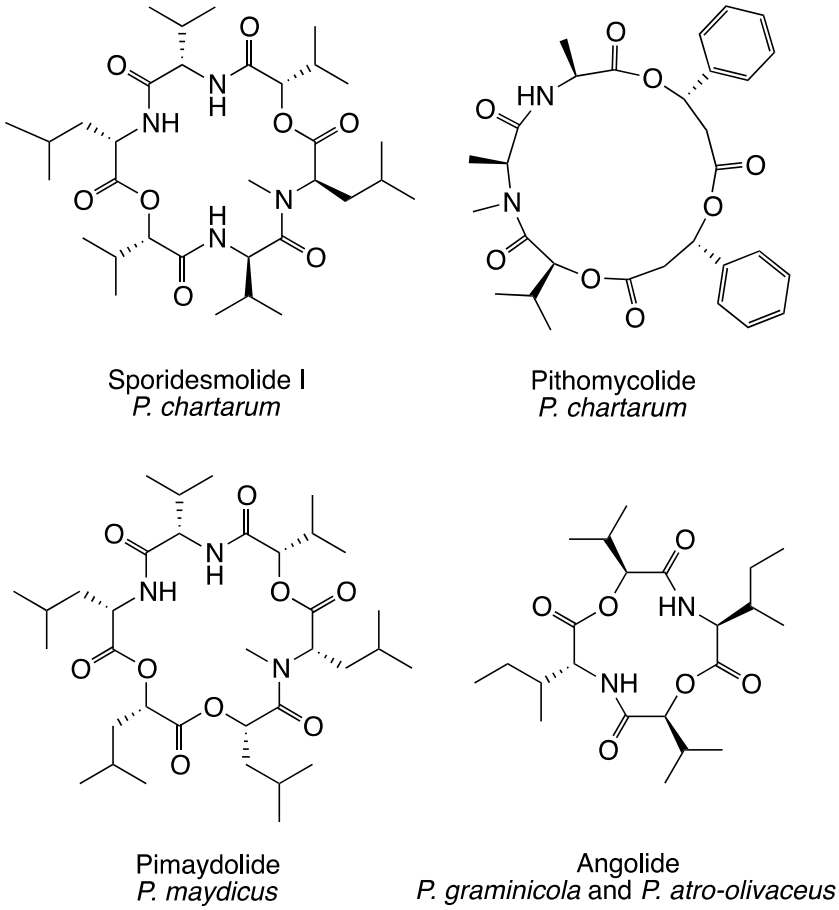

Figure S1. Cyclic depsipeptides from *Pithomyces* and their producing species.

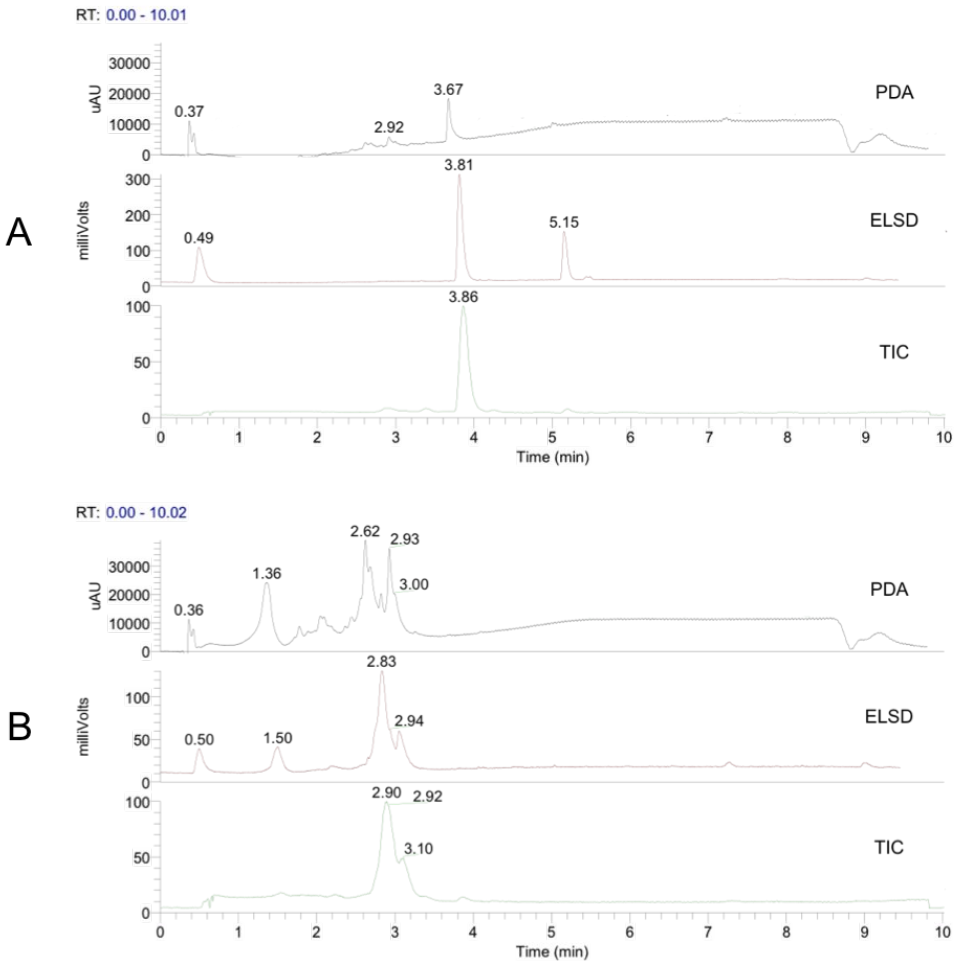

Figure S2. UPLC-HRMS analysis of *Pithomyces* sp. RKDO 1698 EtOAc extracts in addition to ELSD and UV chromatograms. (A) Mycelia extract (**1** elutes at 3.86 min in the TIC) and (B) broth extract.

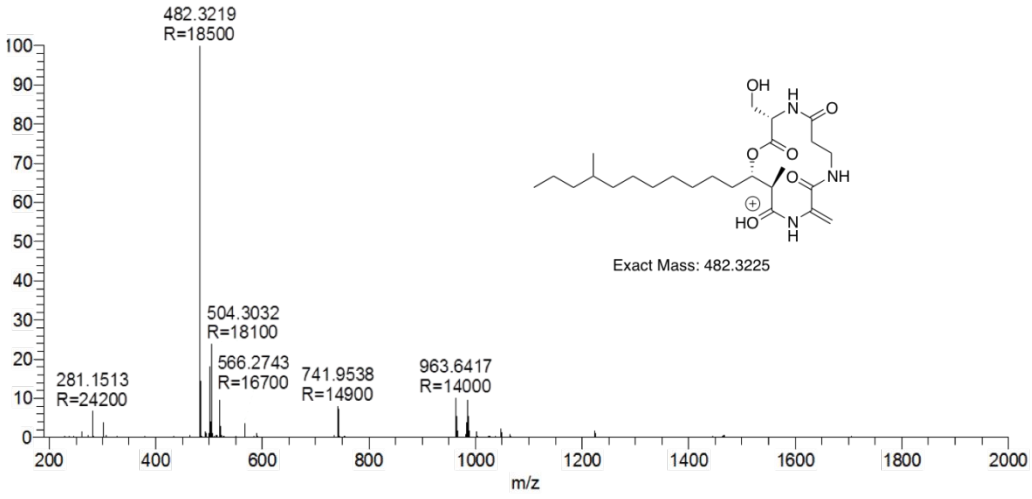

Figure S3. ESI+ HRMS spectrum of **1.**

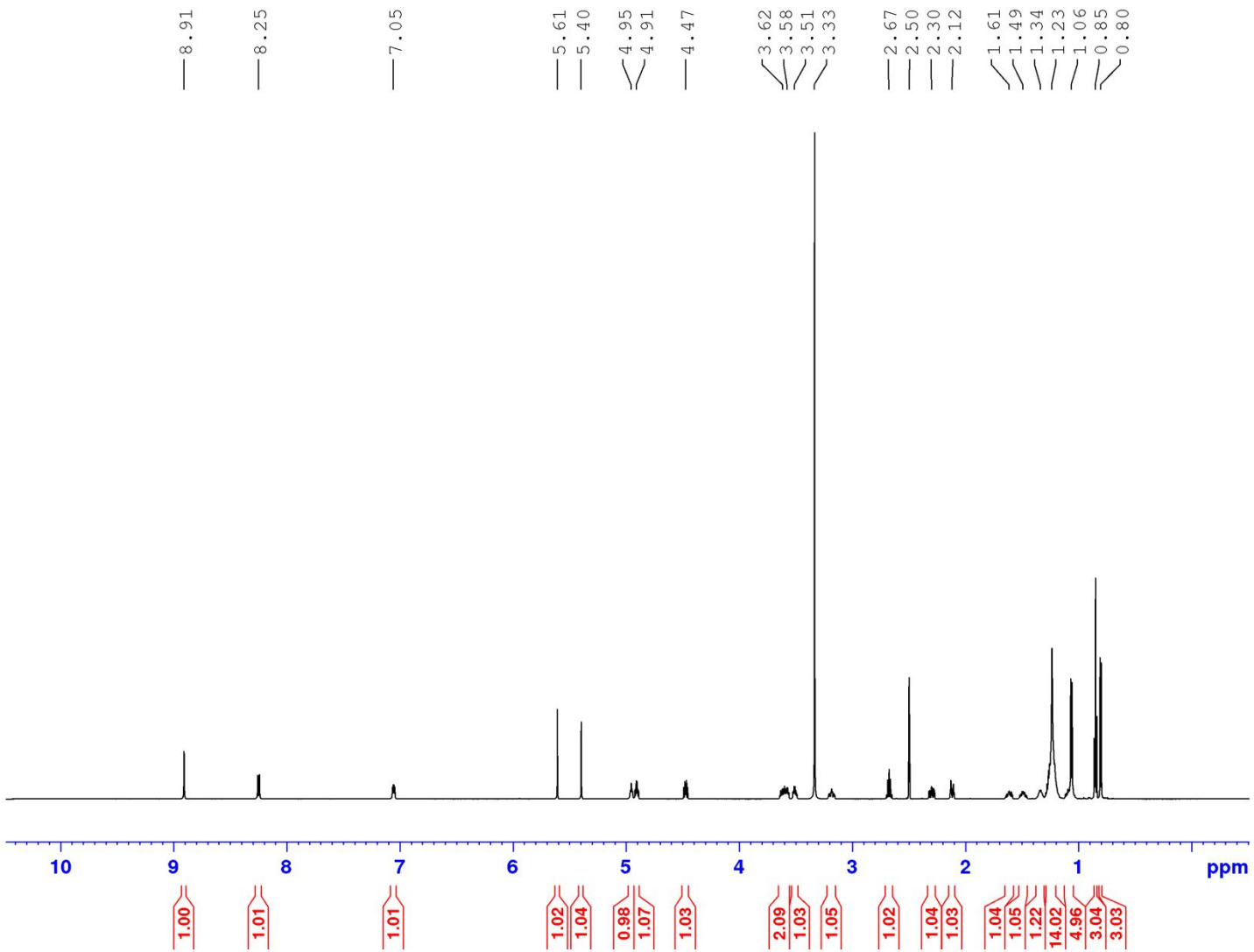

Figure S4. ^{1}H NMR spectrum (600 MHz, DMSO-d_6) of **1**.

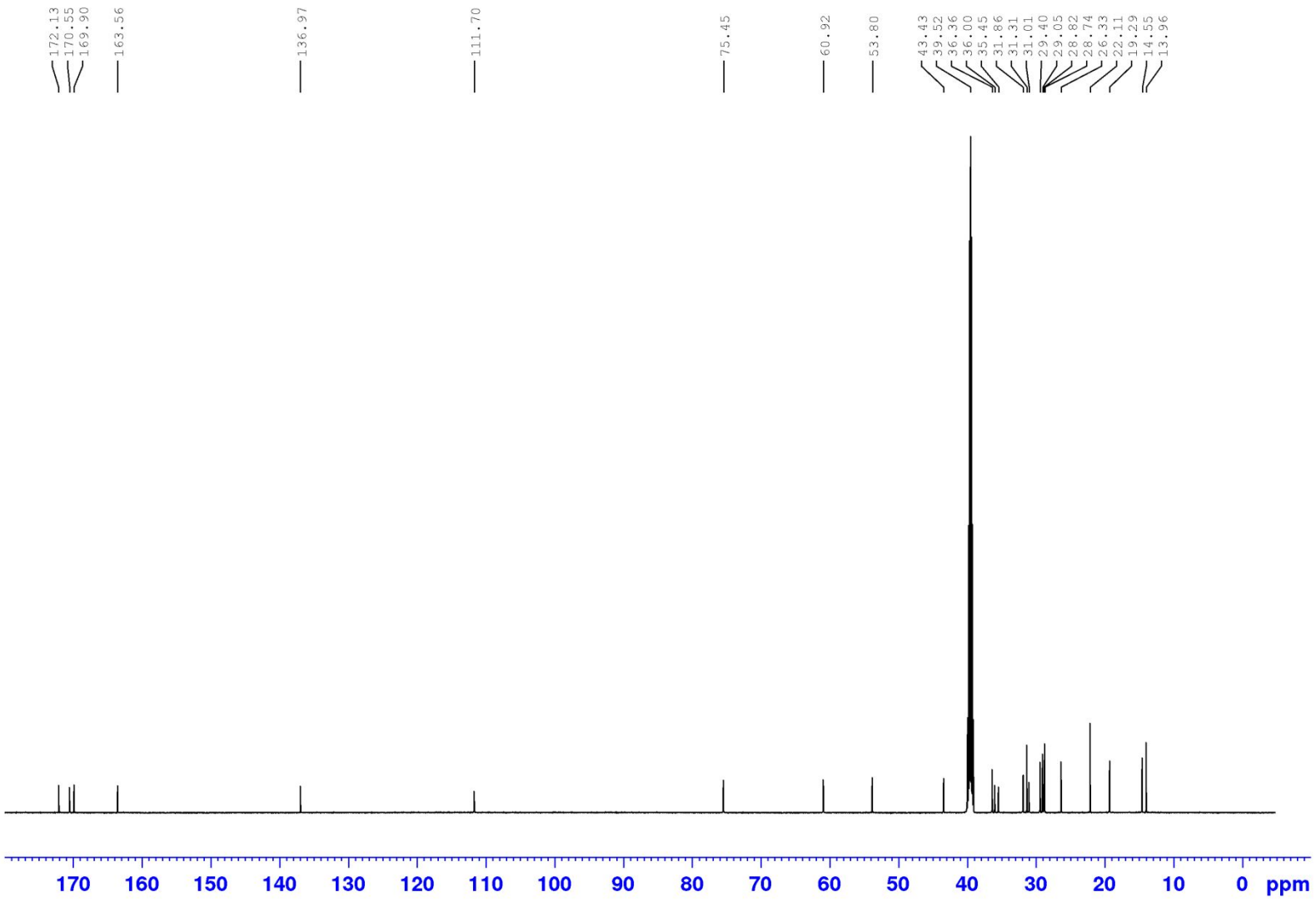

Figure S5. ^{13}C NMR spectrum (600 MHz, DMSO-d_6) of **1**.

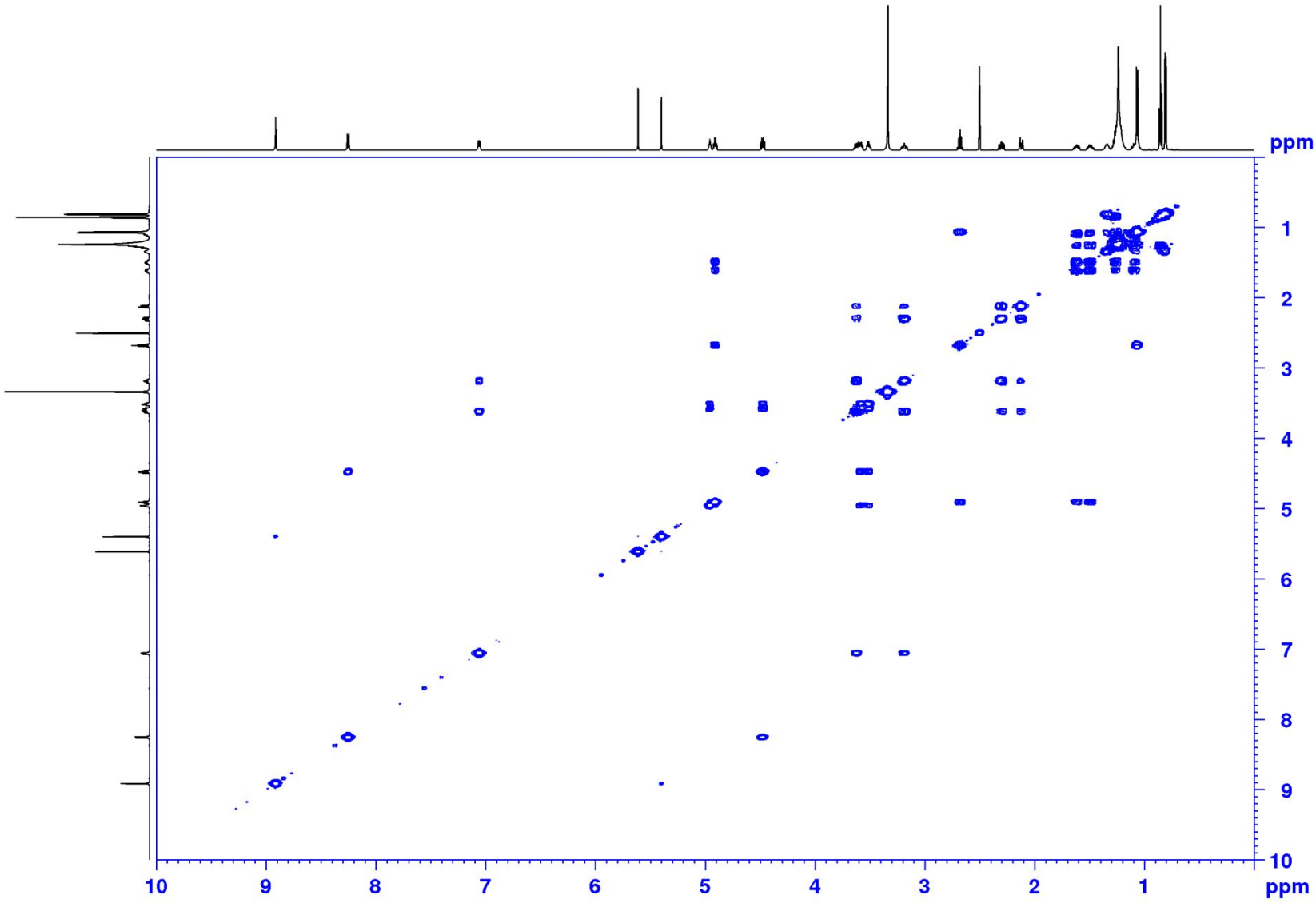

Figure S6. COSY NMR spectrum (600 MHz, DMSO-d_6) of **1**.

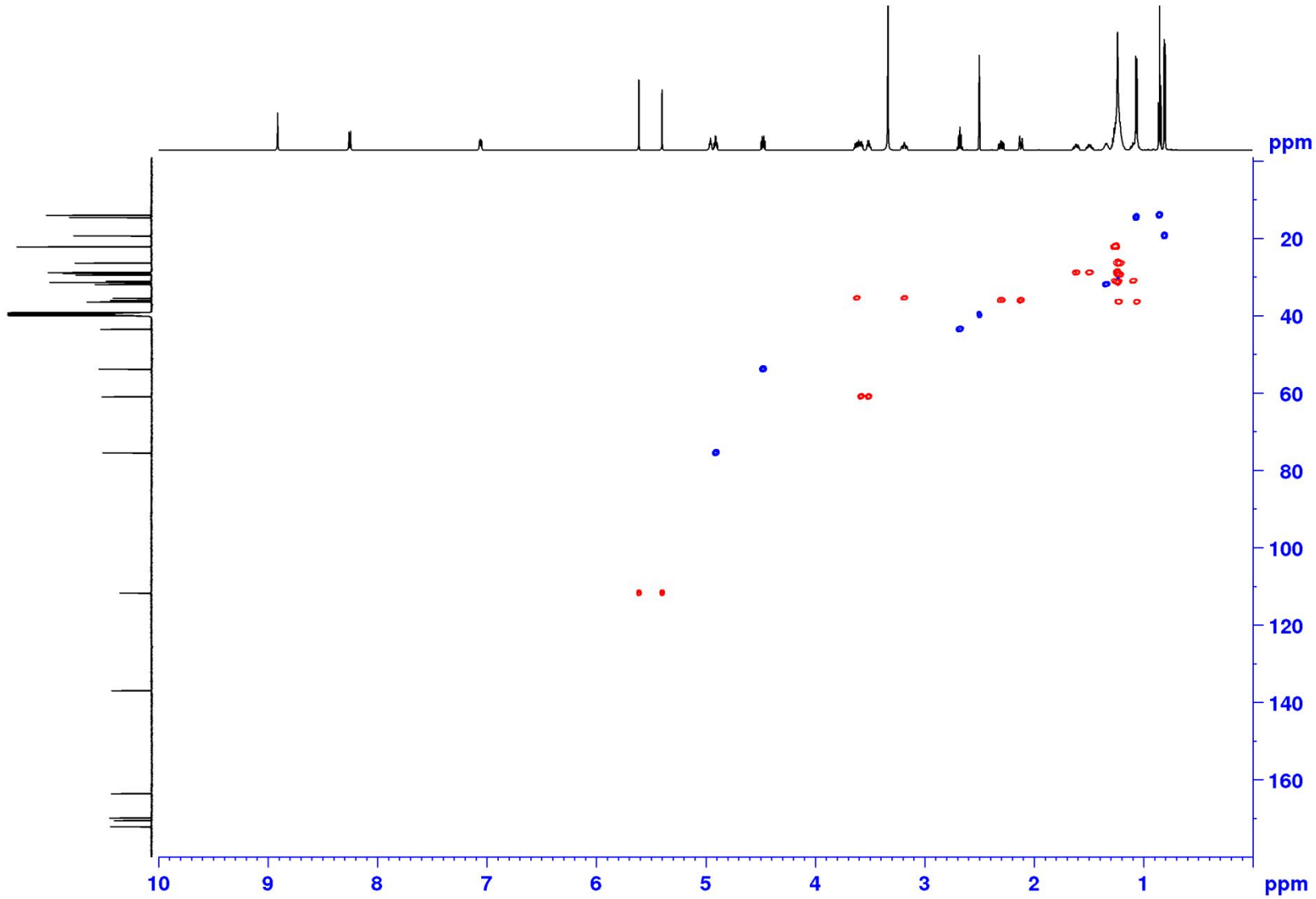

Figure S7. HSQC NMR spectrum (600 MHz, DMSO-d_6) of **1**. Blue contours are positively phased (methyl and methine) and red contours are negatively phased (methylene).

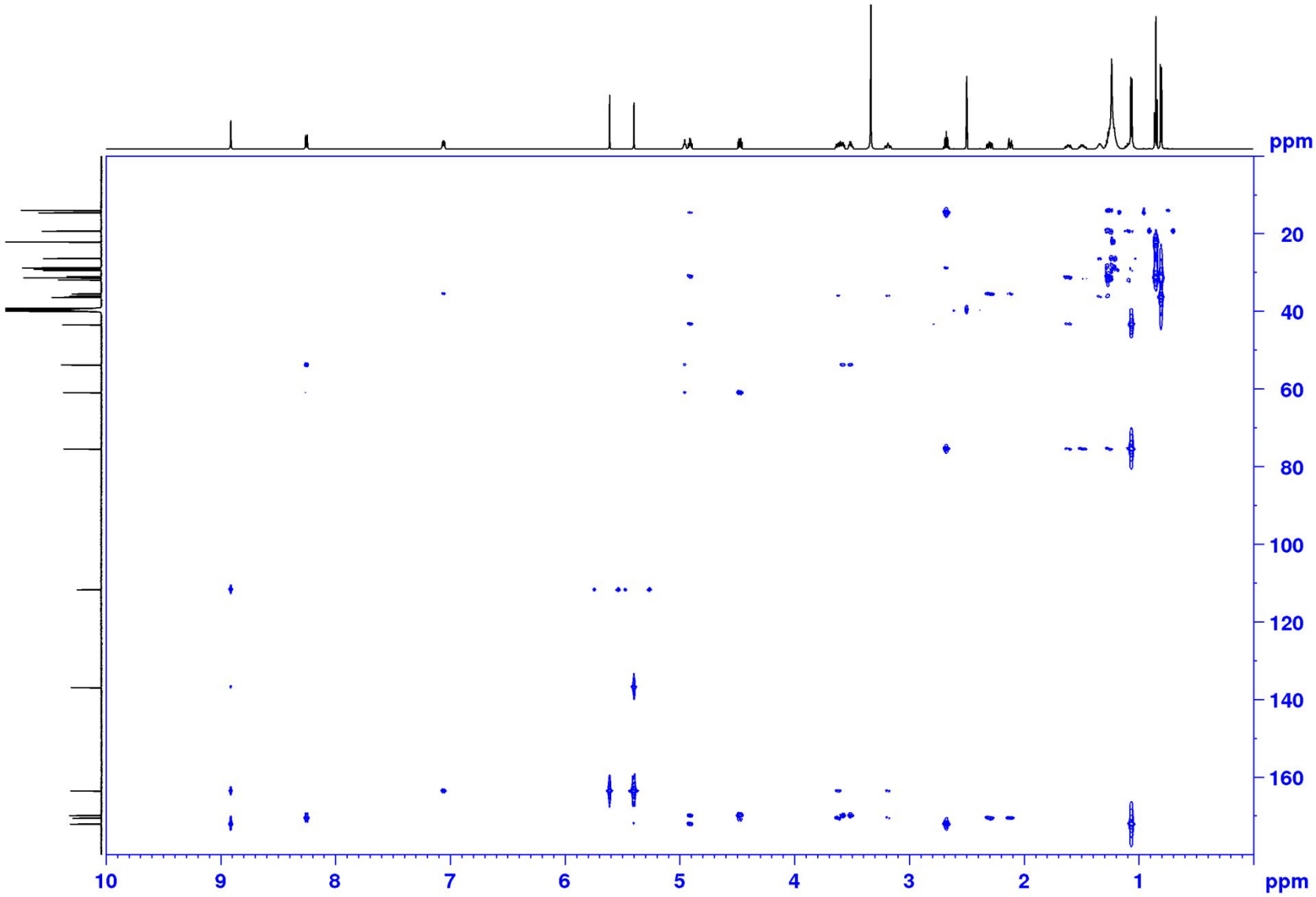

Figure S8. HMBC NMR spectrum (600 MHz, DMSO-d_6) of **1**.

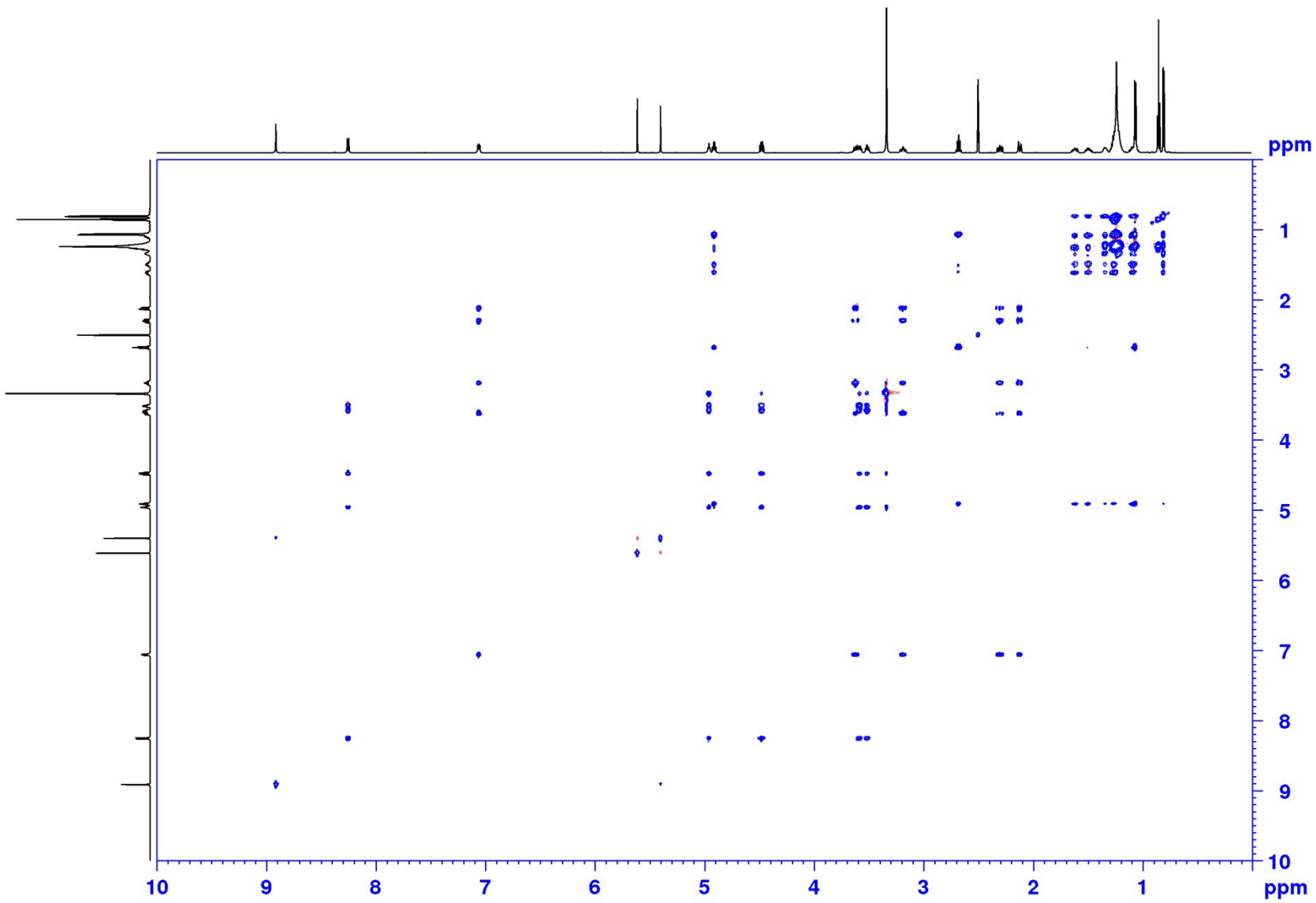

Figure S9. TOCSY NMR spectrum (600 MHz, DMSO-d_6) of **1**.

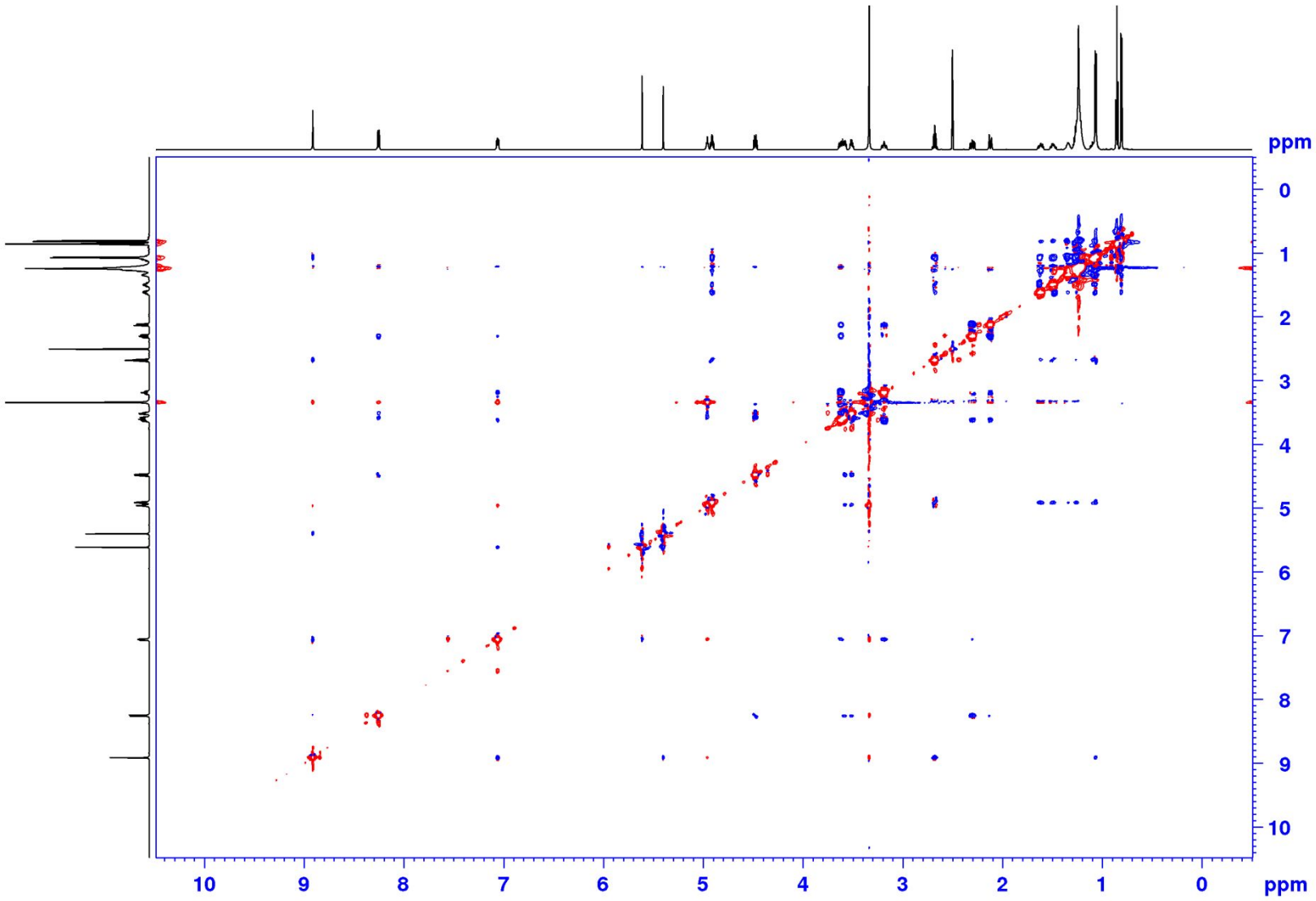

Figure S10. ROESY NMR spectrum (600 MHz, DMSO-d_6) of **1**.

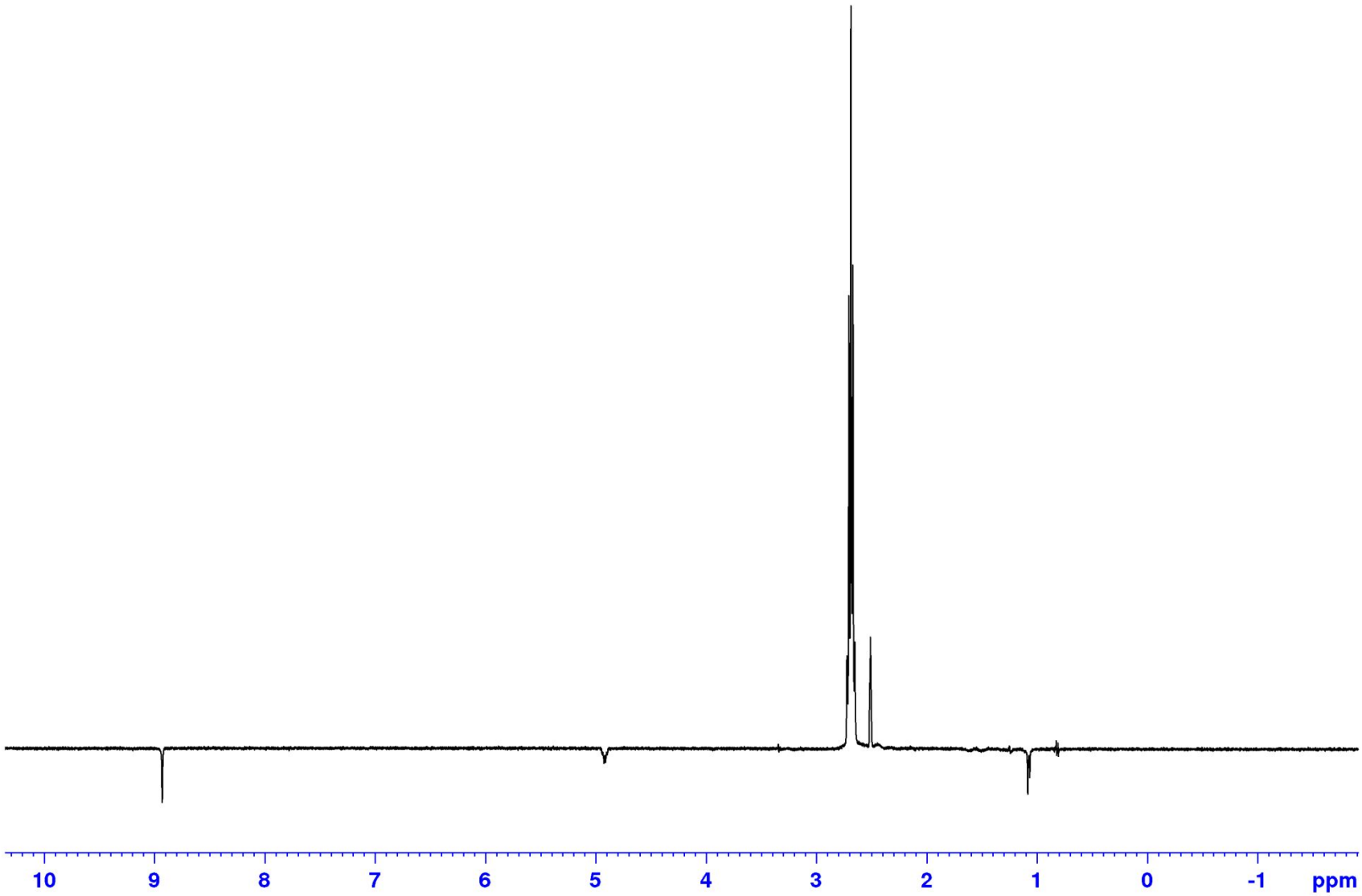

Figure S11. 1D ROESY NMR spectrum (400 MHz, DMSO-d_6) of **1**; H-2 (2.68 ppm) was selectively irradiated. Negatively phased peaks indicate a nOe between the corresponding proton(s) and H-2.

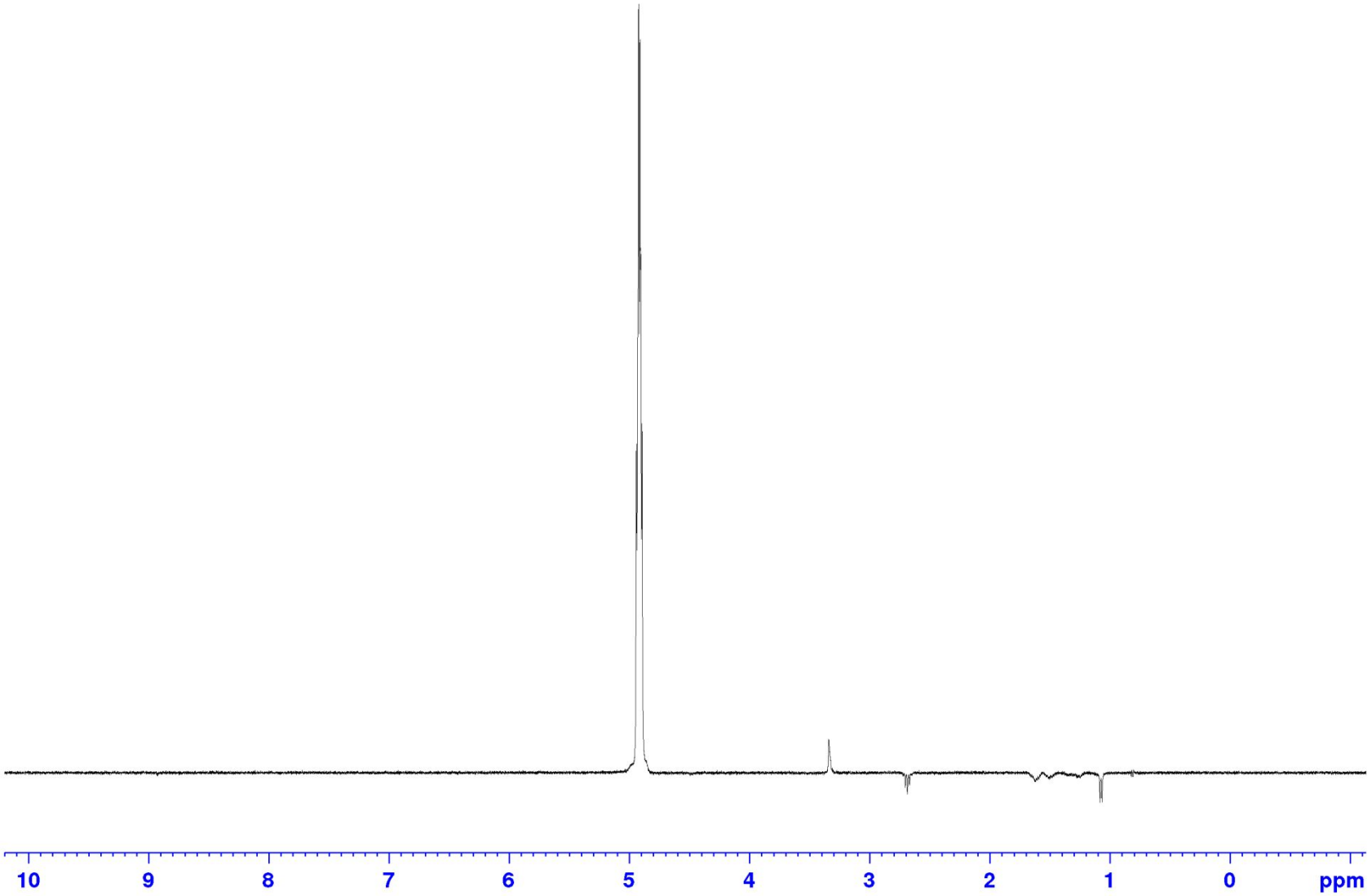

Figure S12. 1D ROESY NMR spectrum (400 MHz, DMSO-d_6) of **1**; H-3 (4.91 ppm) was selectively irradiated. Negatively phased peaks indicate a nOe between the corresponding proton(s) and H-3.

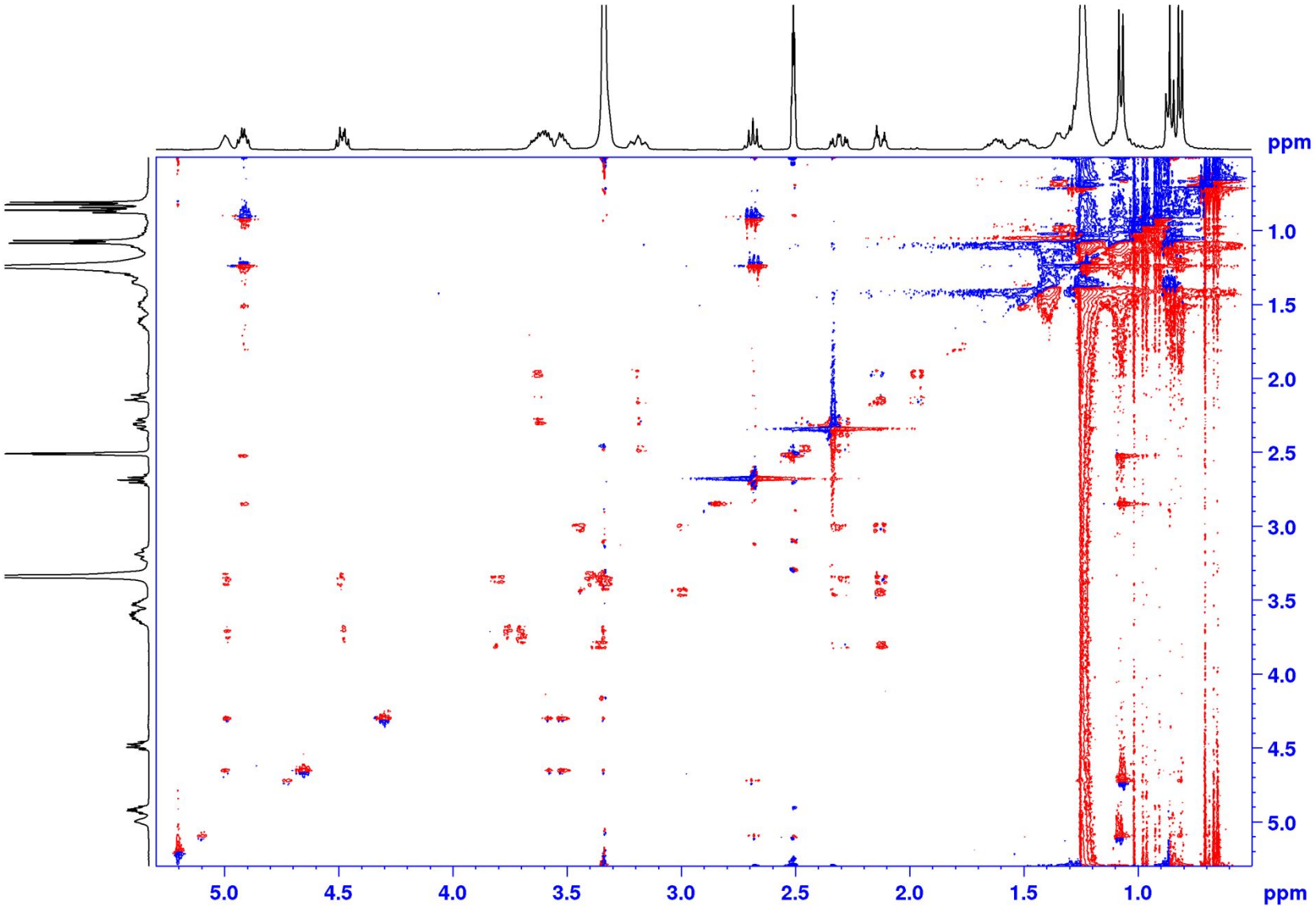

Figure S13. HETLOC NMR spectrum (400 MHz, DMSO-d_6) of **1.**

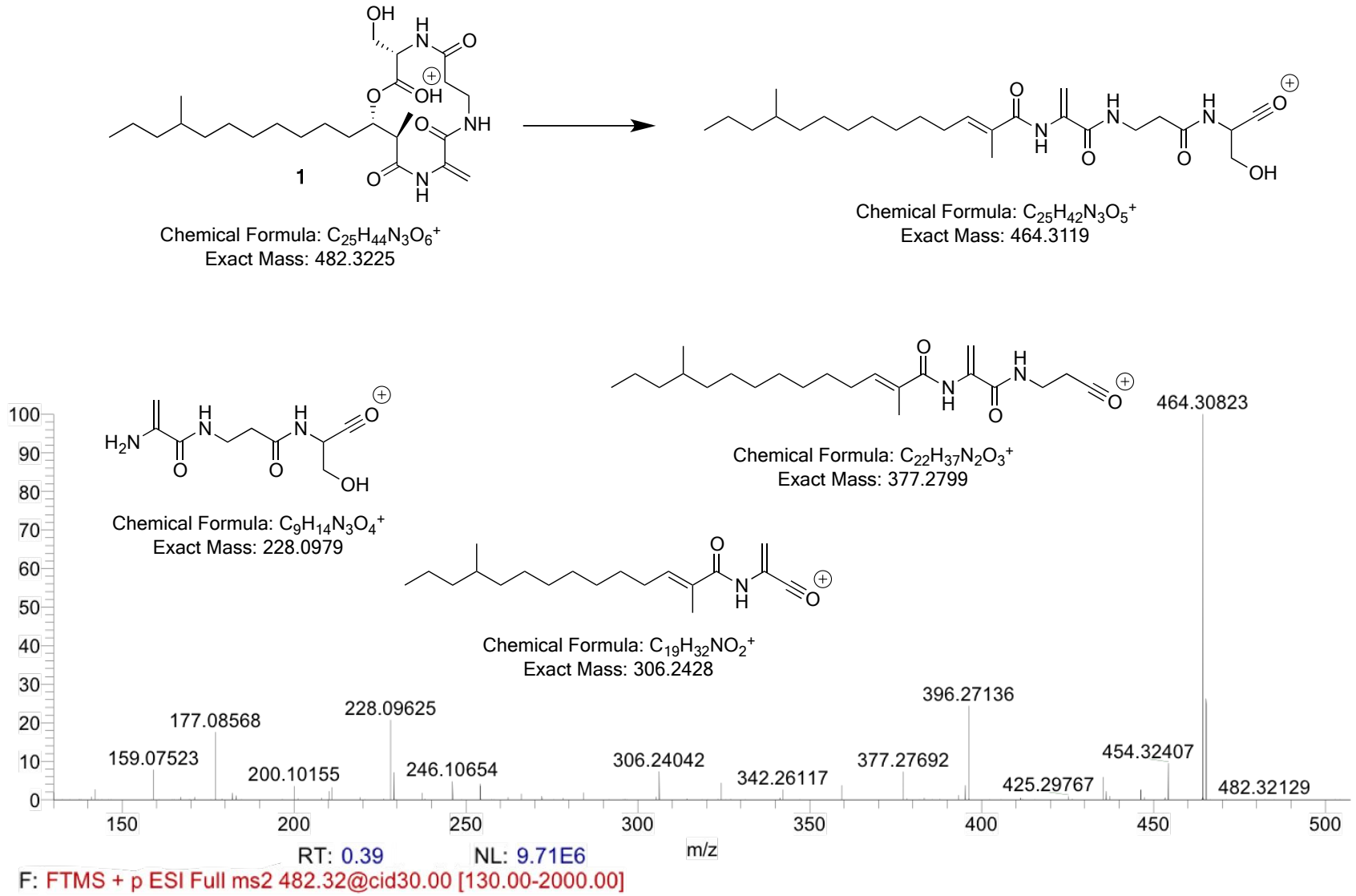

Figure S14. ESI+ MS2 of **1** and select predicted fragments.

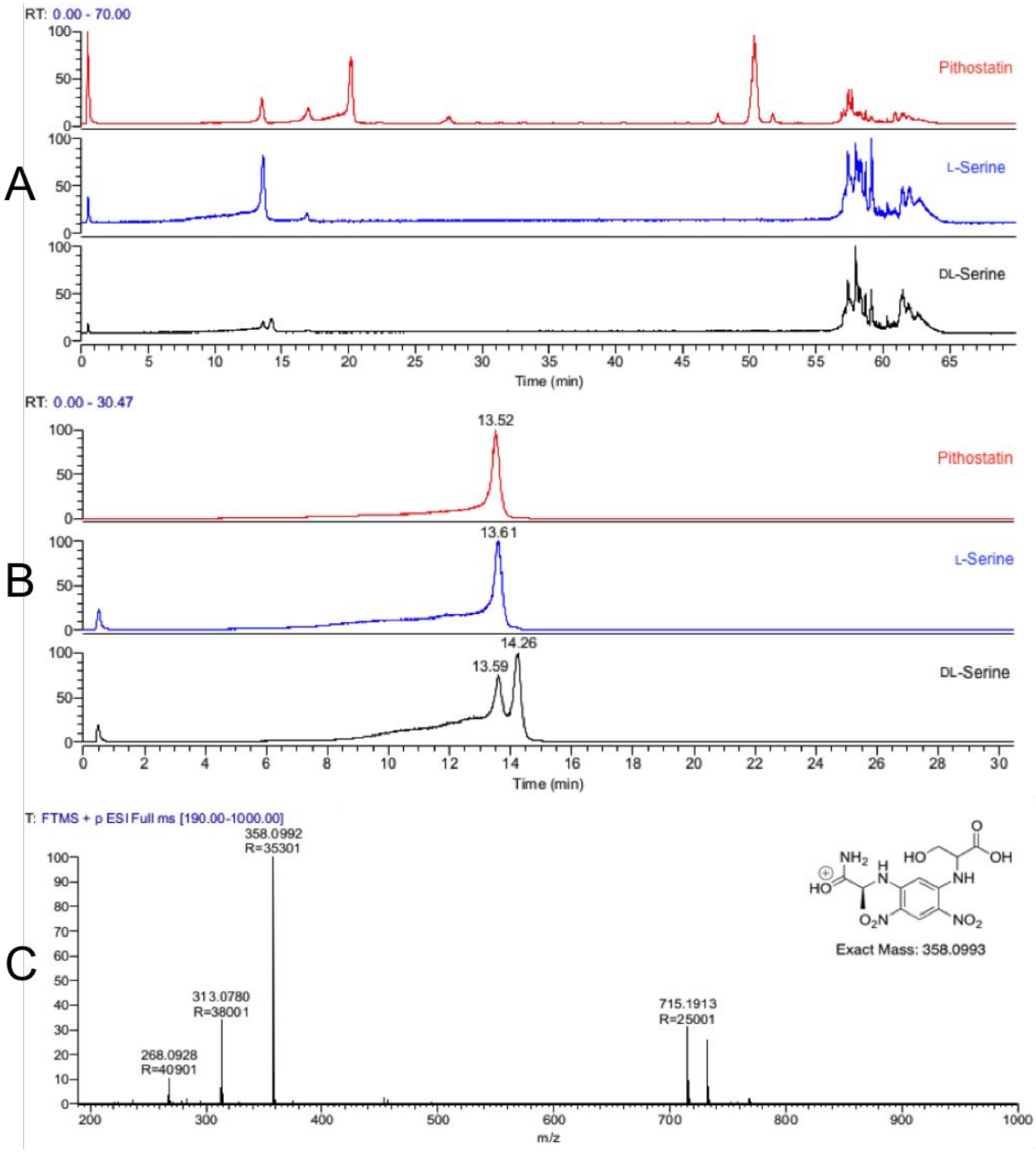

Figure S15. Marfey's analysis of **1**. (A) TIC and (B) XIC 358.0993 ± 10 ppm (retention time window of 0-30 min) for L-FDAA-derivatized serine derived from **1** and from pure serine standards. (C) ESI+ HRMS of L-FDAA-derivatized serine, which is representative of both pure standards and **1** samples.

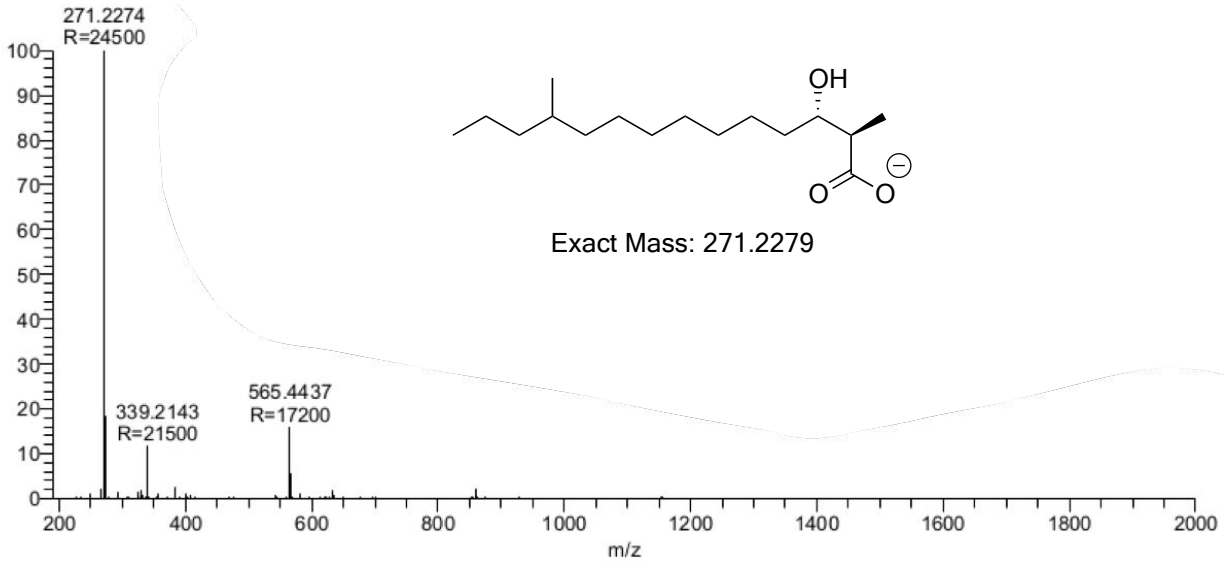

Figure S16. ESI- HRMS spectrum of **6**.

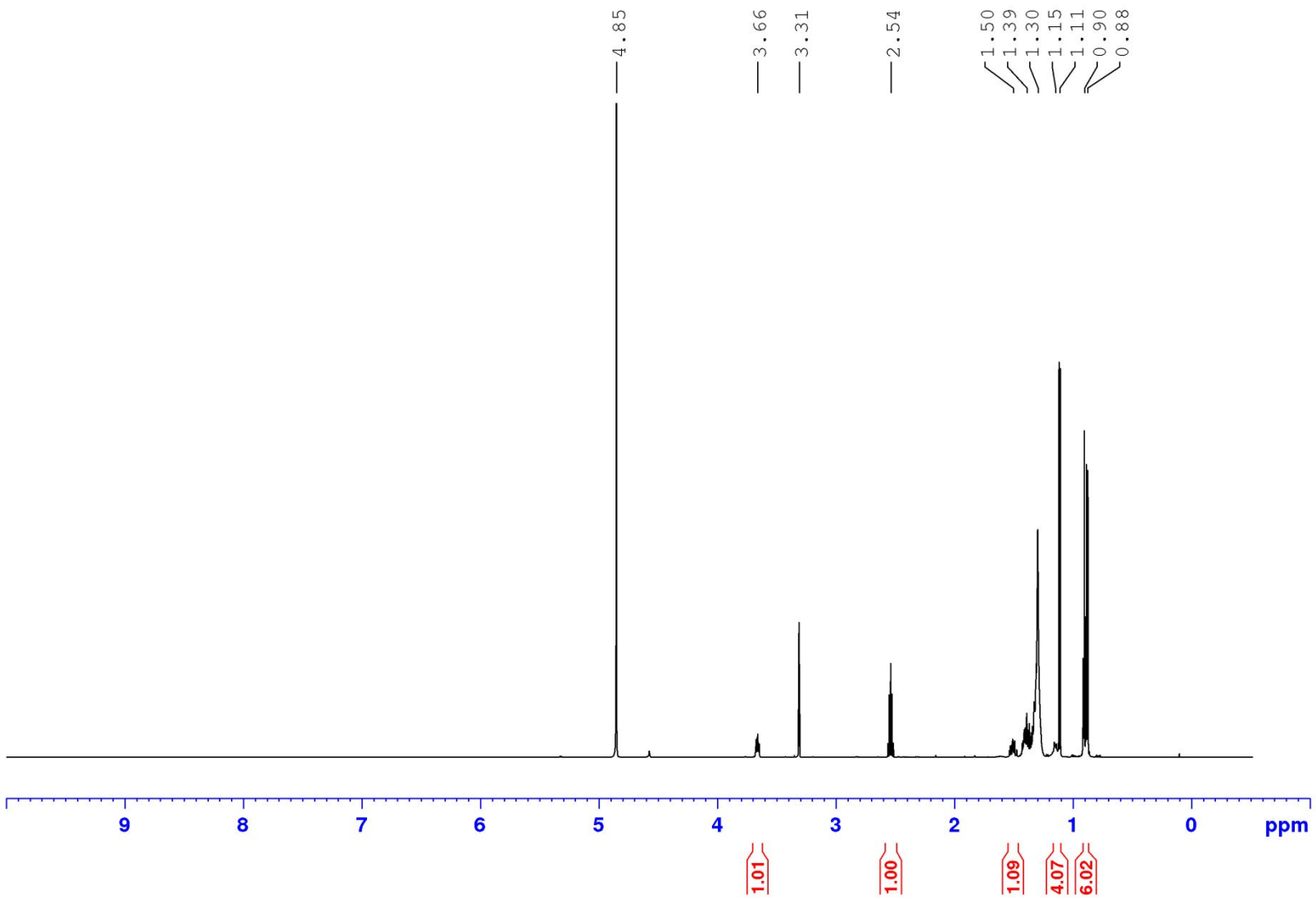

Figure S17. ^{1}H NMR spectrum (600 MHz, CD_3OD) of **6**.

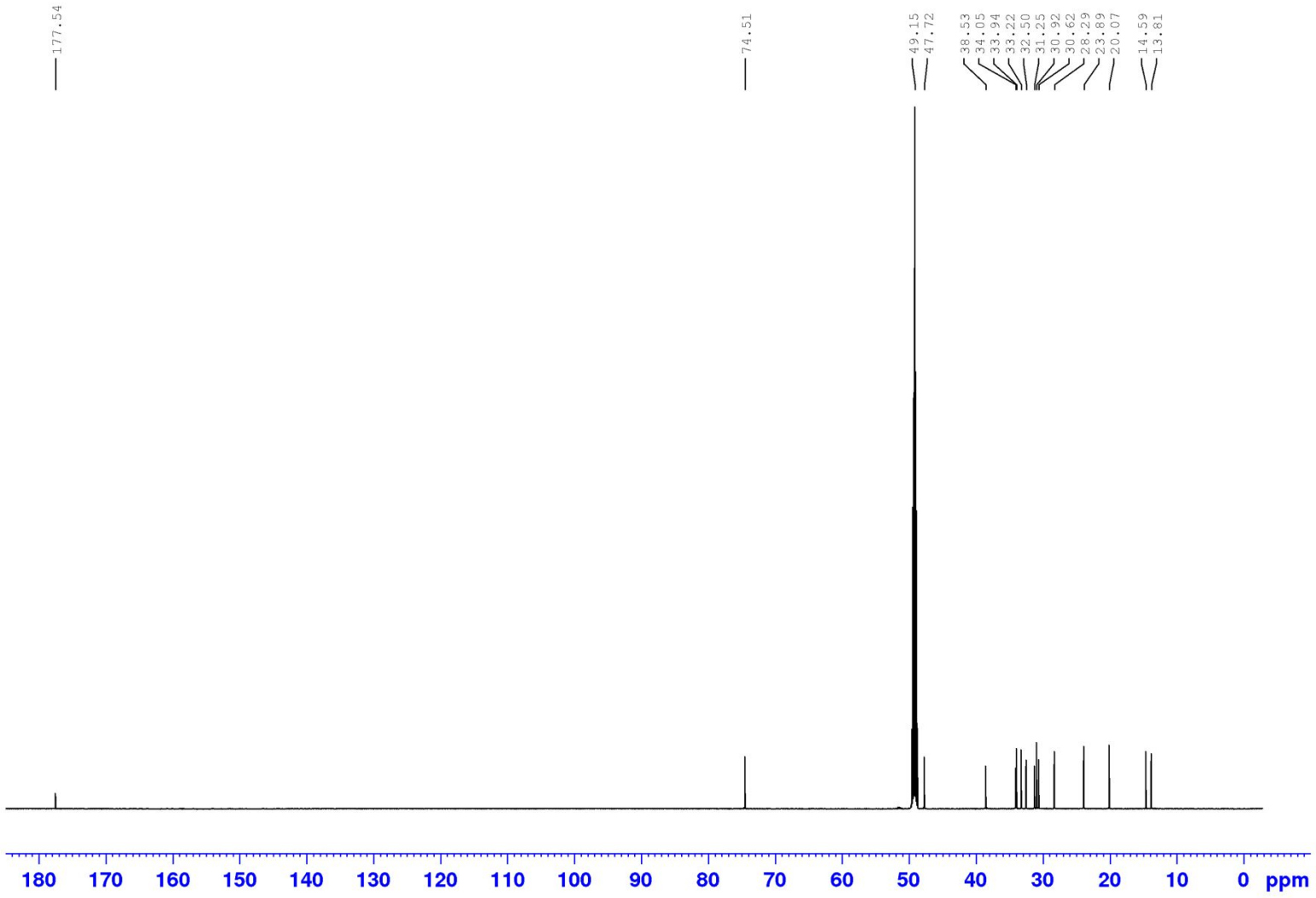

Figure S18. ^{13}C NMR spectrum (600 MHz, CD_3OD) of **6**.

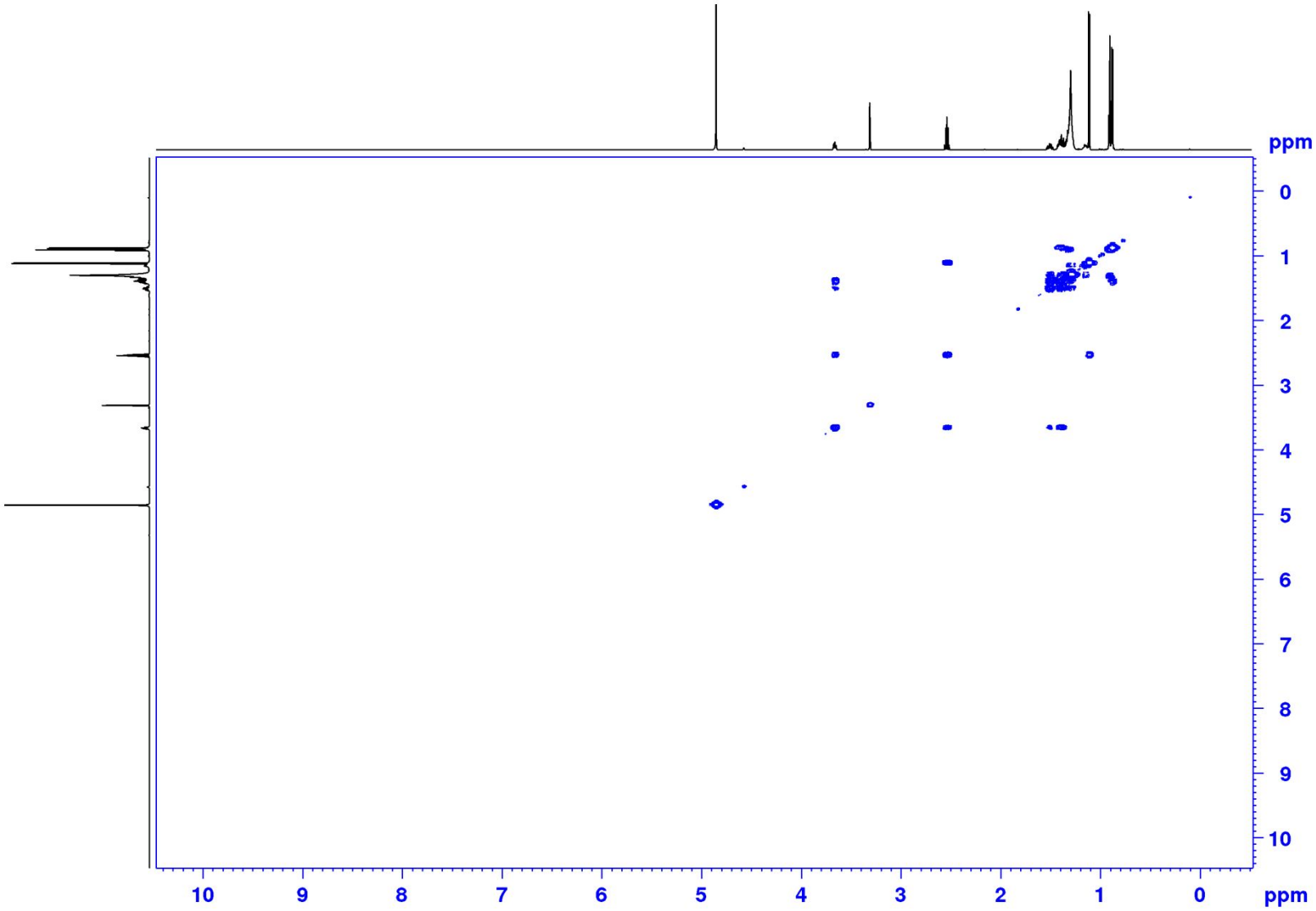

Figure S19. COSY NMR spectrum (600 MHz, CD_3OD) of **6**.

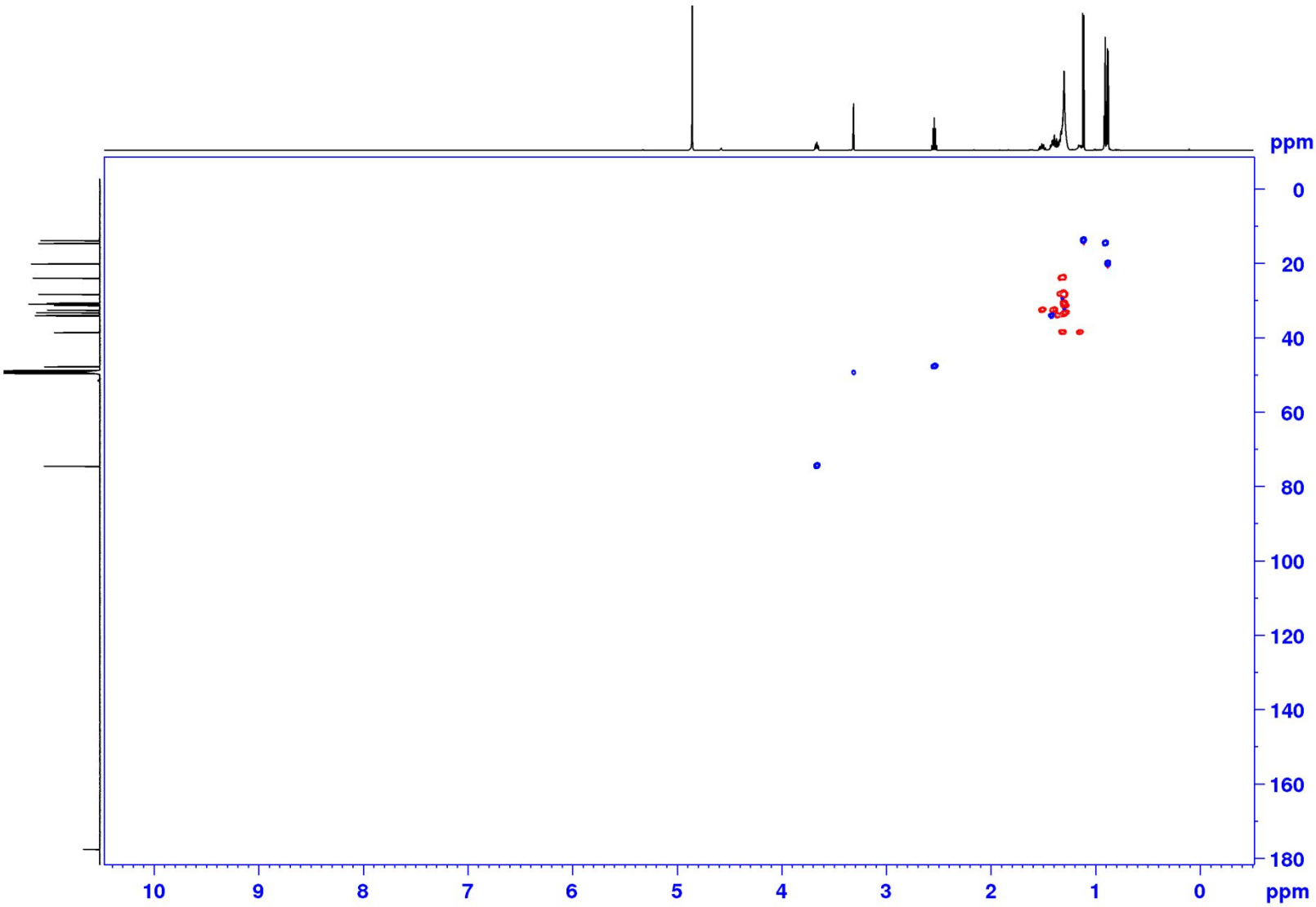

Figure S20. HSQC NMR spectrum (600 MHz, CD_3OD) of **6**. Blue contours are positively phased (methyl and methine) and red contours are negatively phased (methylene).

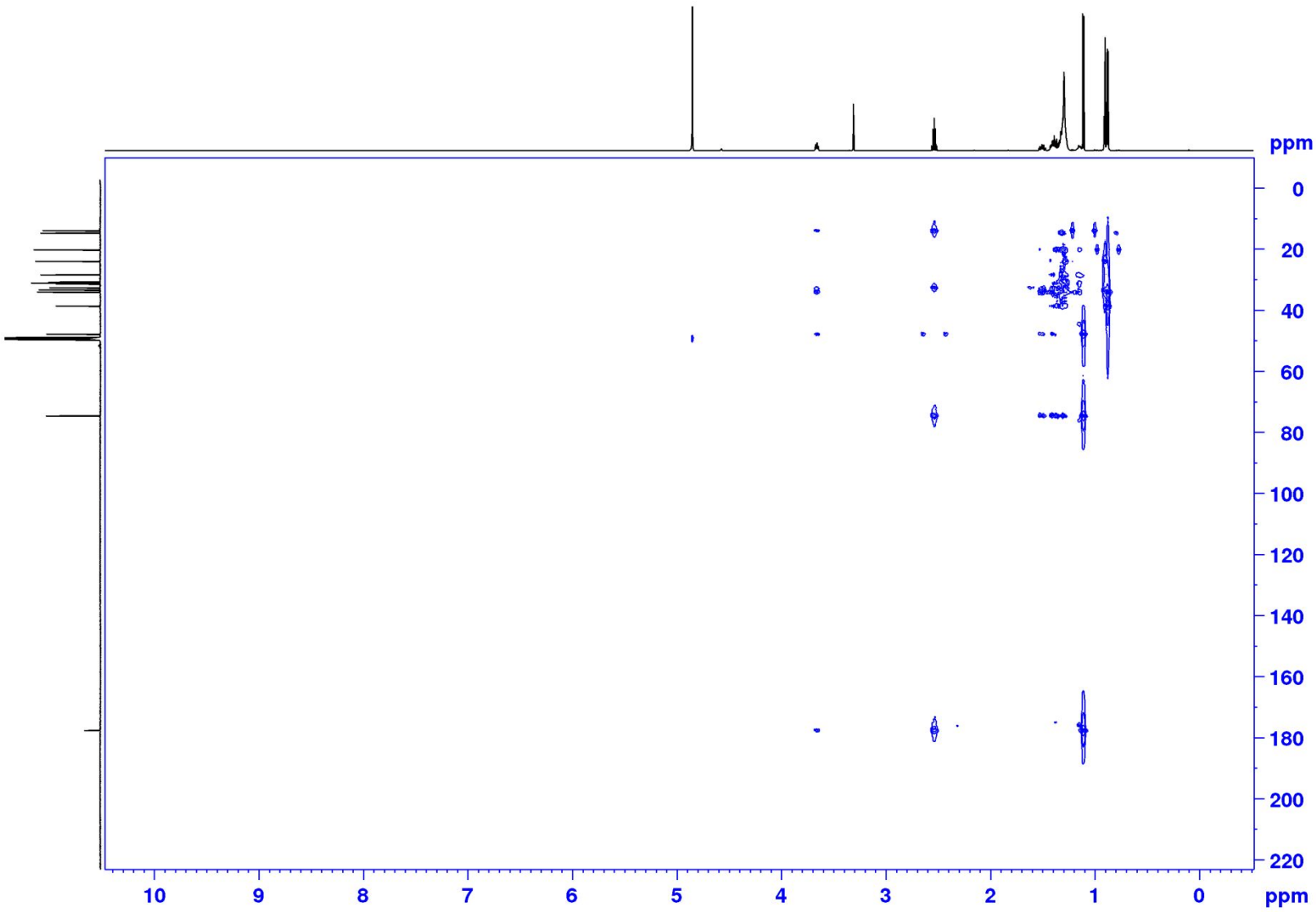

Figure S21. HMBC NMR spectrum (600 MHz, CD_3OD) of **6**.

Table S1. Tabulated NMR spectroscopic data (600 MHz, CD_3OD) for HDMT (6).

Position	δ_C, Type	δ_H, (*J* in Hz)	^1H-^1H COSY	HMBC
1	177.5, C			
2	47.7, CH	2.54, m (7.1)	2-CH_3, 3	1, 2-CH_3, 3, 4
2-CH_3	13.8, CH_3	1.11, d (7.1)	2	1, 2, 3
3	74.5, CH	3.66, td (7.7, 3.3)	2, 4a, 4b	1, 2, 2-CH_3, 5
4	32.5, CH_2	1.39, m	3, 4b	2
	32.5, CH_2	1.5, m	3, 4a	2
5	33.25, CH_2	1.29, m		
6[a]	33.2, CH_2	1.29, m		
7[a]	31.3, CH_2	1.29, m		
8[a]	30.9, CH_2	1.29, m		
9[a]	30.6, CH_2	1.29, m		
10	38.54, CH_2	1.16, m		
	38.54, CH_2	1.31, m		
11	33.9, CH_2	1.41, m		
11-CH_3	20.1, CH_3	0.88, d (6.5)	11	10, 12
12	34.1, CH_2	1.37, m		
13	23.9, CH_2	1.31, m		
14	14.6, CH_3	0.9, t (7.2)	13	12, 13

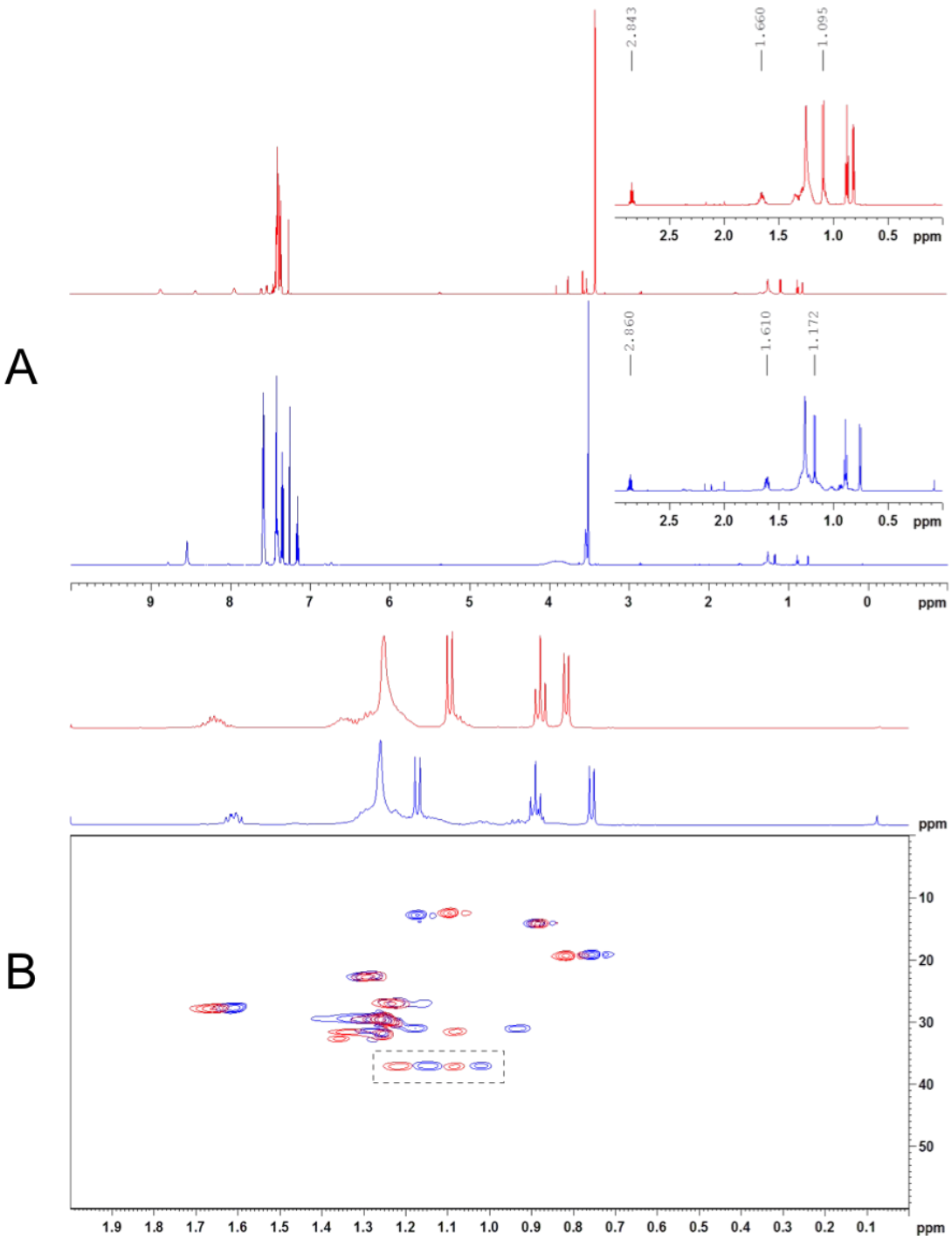

Figure S22. Mosher's ester analysis of **6** cleaved from **1**. (A) ^{1}H NMR spectra and (B) HSQC spectra (both 600 MHz, $CDCl_3$) after reaction with *R*-MTPA-Cl (red) and *S*-MTPA-Cl (blue). HSQC contours corresponding to H4a and H4b are enclosed within the dashed box.

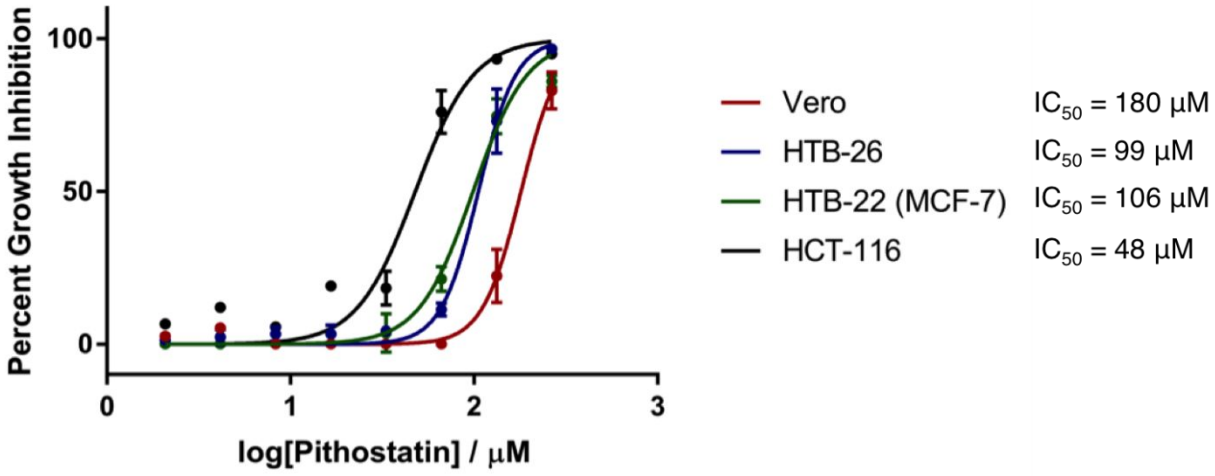

Figure S23. Dose-response curves illustrating results of cytotoxicity assays of **1**. Growth inhibition was observed for one healthy cell line (Vero) and three cancer cell lines (HTB-26, HTB-22 and HCT-116).

Antimicrobial and Cytotoxicity Screening Protocols. Compound **1** was tested for antimicrobial activity against methicillin-resistant *Staphylococcus aureus* ATCC 33591 (MRSA), *S. warneri* ATCC 17917, vancomycin-resistant *Enterococcus faecium* EF379 (VRE), *Pseudomonas aeruginosa* ATCC 14210, *Proteus vulgaris* ATCC 12454, and *Candida albicans* ATCC 14035. All testing was carried out in triplicate according to the Clinical Laboratory Standards Institute testing standards in a 96-well plate microbroth dilution assay as previously described.[20] Optical density was measured using a Thermo Scientific Varioskan Flash plate reader at 600 nm, recording at time zero and then again after incubation for 22 h (37.0 °C) to determine percent growth inhibition. Testing against *Mycobacterium tuberculosis* ATCC25177 was carried out using a previously reported protocol.[21] Fusaristatin C was also tested for cytotoxicity against Vero kidney cell line from African green monkey, adult human epidermal keratinocytes (HEKa), human foreskin BJ fibroblasts, MCF7 human breast adenocarcinoma (ATCC HTB-22), human breast adenocarcinoma cells (ATCC HTB-26) and HCT-116 human colorectal carcinoma cells (ATCC CCL-247). All assays were carried out as described previously.[20] Fluorescence was measured using a Thermo Scientific Varioskan Flash plate reader at 560/12 excitation, 590 nm emission both at time zero and 4 h after Alamar blue addition in order to calculate IC_{50} values.

(20) Overy, D. P.; Berrue, F.; Correa, H.; Hanif, N.; Hay, K.; Lanteigne, M.; McQuillan, K.; Duffy, S.; Boland, P.; Jagannathan, R.; Carr, G. S.; Vansteeland, M.; Kerr, R. G. *Mycology* **2014**, *5* (3), 130–144.

(21) Collins, L.; Franzblau, S. G. *Antimicrob. Agents Chemother.* **1997**, *41* (5), 1004–1009.